Heptanuclear Antiferromagnetic Fe(III)−D-(-)-Quinato Assemblies with an $S = 3/2$ Ground State—pH-Specific Synthetic Chemistry, Spectroscopic, Structural, and Magnetic Susceptibility Studies

M. Menelaou,[†,#] E. Vournari,[†] V. Psycharis,[‡] C. P. Raptopoulou,[‡] A. Terzis,[‡] V. Tangoulis,[§] Y. Sanakis,[‡] C. Mateescu,[∥] and A. Salifoglou*,[†]

[†]Laboratory of Inorganic Chemistry, Department of Chemical Engineering, Aristotle University of Thessaloniki, Thessaloniki 54124, Greece

[‡]Institute of Advanced Materials, Physicochemical Processes, Nanotechnology and Microsystems, Department of Materials Science, NCSR "Demokritos", Aghia Paraskevi, 15310 Attiki, Greece

[§]Department of Chemistry, Aristotle University of Thessaloniki, Thessaloniki 54124, Greece

[∥]Banat's University of Agricultural Sciences and Veterinary Medicine from Timisoara, Timisoara 300645, Romania

Ⓢ *Supporting Information*

ABSTRACT: Iron is an essential metal ion with numerous roles in biological systems and advanced abiotic materials. D-(-)-Quinic acid is a cellular metal ion chelator, capable of promoting reactions with metal M(II,III) ions under pH-specific conditions. In an effort to comprehend the chemical reactivity of well-defined forms of Fe(III)/Fe(II) toward α-hydroxycarboxylic acids, pH-specific reactions of: (a) $[Fe_3O(CH_3COO)_6(H_2O)_3]\cdot(NO_3)\cdot4H_2O$ with D-(-)-quinic acid in a molar ratio 1:3 at pH 2.5 and (b) Mohr's salt with D-(-)-quinic acid in a molar ratio 1:3 at pH 7.5, respectively, led to the isolation of the first two heptanuclear Fe(III)−quinato complexes, $[Fe_7O_3(OH)_3(C_7H_{10}O_6)_6]\cdot20.5H_2O$ (**1**) and $(NH_4)[Fe_7(OH)_6(C_7H_{10}O_6)_6]\cdot(SO_4)_2\cdot18H_2O$ (**2**). Compounds **1** and **2** were characterized by analytical, spectroscopic (UV−vis, FT-IR, EPR, and Mössbauer) techniques, CV, TGA-DTG, and magnetic susceptibility measurements. The X-ray structures of **1** and **2** reveal heptanuclear assemblies of six Fe(III) ions bound by six doubly deprotonated quinates and one Fe(III) ion bound by oxido- and hydroxido-bridges (**1**), and hydroxido-bridges (**2**), all in an octahedral fashion. Mössbauer spectroscopy on **1** and **2** suggests the presence of Fe(III) ions in an all-oxygen environment. EPR measurements indicate that **1** and **2** retain their structure in solution, while magnetic measurements reveal an overall antiferromagnetic behavior with a ground state $S = 3/2$. The collective physicochemical properties of **1** and **2** suggest that the (a) nature of the ligand, (b) precursor form of iron, (c) pH, and (d) molecular stoichiometry are key factors influencing the chemical reactivity of the binary Fe(II,III)-hydroxycarboxylato systems, their aqueous speciation, and ultimately through variably emerging hydrogen bonding interactions, the assembly of multinuclear Fe(III)−hydroxycarboxylato clusters with distinct lattice architectures of specific dimensionality (2D−3D) and magnetic signature.
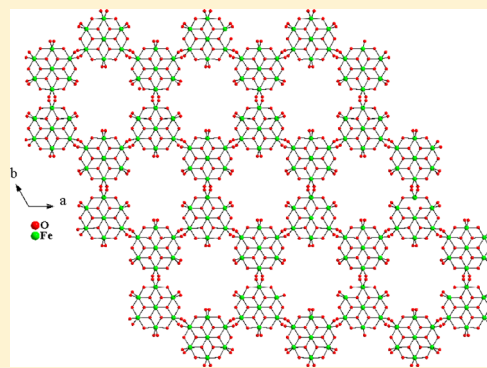
INTRODUCTION

Over the last decades, research activities have focused on the synthesis and characterization of polynuclear cluster compounds of magnetic transition metal ions,[1] such as manganese[2−4] and iron.[5,6] The main reasons for this attractive research interest are due to the potential applications of the arising materials as molecular magnets (e.g., SMMs), exhibiting hysteresis and slow magnetic relaxation behavior.[7−9] Iron is an important transition metal ion found in many biological systems in all living organisms.[10−13] It is ubiquitous in the environment and participates in a wide range of material processes involving alloys, catalysts, and dye-casting. Metal ions such as iron are mobilized in various abiotic systems through interactions with appropriately structured organic ligands acting

as chelates. In this regard, organic ligands bearing O-, N-, and S-containing anchors are excellent candidates, interacting with transition metal ions and leading to the isolation of polynuclear clusters. As a result, hydroxido-, alkoxido-, and/or phenoxido-type O-ligands have been widely used in the synthesis of polynuclear species with intriguing lattice architecture (wheel-like structures,[14−17] diamond-like structures[18]) and distinctly remarkable magnetic properties.

A very efficient low molecular mass O-chelator ligand is D-(-)-quinic acid, $1\alpha,3\alpha,4\alpha,5\beta$-tetrahydroxy-1-cyclohexane carboxylic acid, encountered as a vital binder in plant cellular

physiology. It is a precursor of shikimic acid,[19] which is involved in the biosynthesis of many natural products including essential amino acids and folic acid.[20,21] It is a multifunctional binder with versatile coordination modes containing important features: (a) a carboxylate moiety, known to promote metal ion binding, (b) one alcoholic group in a position α- to the carboxylate group, and (c) three additional alcoholic groups relevant to polyol functionalities. These structural attributes are very essential in promoting diverse metal-ion-binding chemistries in aqueous media. In this regard, the paucity of well-defined and characterized binary multinuclear M(II,III)−quinato species in aqueous media with unique physicochemical properties, such as Fe(III)−quinic acid species, has initiated research efforts in our laboratories, targeting synthetic and solution studies. To this end, exploration of the binary Fe(II,III)−D-(-)-quinic acid system aims at (a) unravelling key aspects of the structural speciation of the aforementioned system, (b) pursuing variable synthetic strategies toward the synthesis of novel binary/ternary materials, and (c) delineating reactivity and physicochemical properties in the solid state and in solution, thereby shedding light on the magnetic properties and establishing magnetostructural correlations in large binary ferric−ligand assemblies. To this end, we herein report on the pH-specific synthesis and isolation of the first two binary heptanuclear Fe(III)−quinato species with an antiferromagnetic ground state $S = 3/2$, bearing distinct lattice architecture and spectroscopic properties, and shedding light onto intertwined factors correlating aqueous solution chemical reactivity and solid state properties in iron−oxido assemblies.

■ EXPERIMENTAL SECTION

Materials and Methods. All experiments were carried out in aqueous media under aerobic conditions. Nanopure-quality water was used for all reactions. $Fe(NO_3)_3 \cdot 9H_2O$ and D-(-)-quinic acid (Fluka), $(NH_4)_2Fe(SO_4)_2 \cdot 6H_2O$ (Merck), $CH_3COONa \cdot 3H_2O$ (Mallinckrodt), and ammonia (Aldrich) were used in this investigation and obtained from commercial suppliers.

Physical Measurements. FT-infrared spectra were recorded on a Perkin-Elmer 1760X FT-infrared spectrometer. UV−vis measurements were carried out on a Hitachi U2001 spectrophotometer in the range from 190 to 1000 nm. A ThermoFinnigan Flash EA 1112 CHNS elemental analyzer was used for the simultaneous determination of carbon, hydrogen, and nitrogen (%). A TA Instruments (model Q 600) system was used to run the simultaneous TGA-DTG experiments.

The EPR spectra of **1** and **2** in the solid state and in aqueous solutions were recorded on a Bruker ER 200D-SRC X-band spectrometer, equipped with an Oxford ESR 9 cryostat at 9.61 GHz, 10 dB (2 mW), and 4 K. Magnetic susceptibility data were collected on powdered samples of **1** and **2** with a Quantum Design SQUID susceptometer in the 2−300 K temperature range, under various applied magnetic fields. Magnetization measurements were carried out at three different temperatures in the field range of 0−5 T.

Zero-field Mössbauer spectra from polycrystalline samples of **1** and **2** were recorded with the conventional constant acceleration method, using a $^{57}Co/Rh$ source and an Oxford cryostat. Samples for Mössbauer spectroscopy were prepared by grinding single crystals in liquid nitrogen.

Electrochemical measurements were carried out with a model PGSTAT30 potensiostat−galvanostat from Autolab Electrochemical Instruments. The entire system was under computer control and supported by the appropriate computer software GPES, running on Windows XP. The employed electrochemical cell had platinum (disk) working and auxiliary (wire) electrodes. A Ag/AgCl electrode was used as reference electrode. KNO_3 was used as a supporting electrolyte. Normal concentrations used were 1−6 mM in electroanalyte and 0.1

M in supporting electrolyte. Purified argon was used to purge the solutions prior to the electrochemical measurements.

Synthesis of $[Fe_3O(CH_3COO)_6(H_2O)_3] \cdot (NO_3) \cdot 4H_2O$. The synthesis and isolation was carried out according to the literature.[22]

Synthesis of $[Fe_7O_3(OH)_3(C_7H_{10}O_6)_6] \cdot 20.5H_2O$ (1). A quantity of $[Fe_3O(CH_3COO)_6(H_2O)_3] \cdot (NO_3) \cdot 4H_2O$ (0.15 g, 0.21 mmol) was placed in a flask and dissolved in 4 mL of H_2O. To that solution, D-(-)-quinic acid (0.12 g, 0.63 mmol) was added slowly and under continuous stirring, and the pH of the solution was 2.5. The resulting reaction solution was stirred for 1 h at room temperature, with the color turning brownish and staying on as such. Subsequently, the reaction mixture was placed at 4 °C and left undisturbed. A few months later, brownish crystals appeared at the bottom of the flask. The crystals were isolated by filtration and dried in vacuo. The yield was 0.10 g (∼56%). Formula: $C_{42}H_{104}Fe_7O_{62.50}$. $M_r = 2000.20$. Anal. Calcd for (**1**) $[Fe_7O_3(OH)_3(C_7H_{10}O_6)_6] \cdot 20.5H_2O$: C, 25.19; H, 5.20. Found: C, 25.03; H, 5.30%.

Synthesis of $(NH_4)[Fe_7(OH)_6(C_7H_{10}O_6)_6] \cdot (SO_4)_2 \cdot 18H_2O$ (2). A quantity of Mohr's salt $((NH_4)_2Fe(SO_4)_2 \cdot 6H_2O)$ (0.20 g, 0.50 mmol) was placed in a flask and dissolved in 4 mL of H_2O. To that solution, D-(-)-quinic acid (0.29 g, 1.5 mmol) was added slowly and under continuous stirring. Aqueous ammonia was then added slowly to adjust the pH to a final value of 7.5. The color of the solution was greenish and stayed on as such. Subsequently, ethanol was added and the reaction mixture was placed at 4 °C. A few weeks later, crystals appeared at the bottom of the flask. The crystals were isolated by filtration and dried in vacuo. The yield was 0.12 g (∼78%). Formula: $C_{42}H_{106}Fe_7NO_{68}S_2$. $M_r = 2168.35$. Anal. Calcd for (**2**) $(NH_4)-[Fe_7(OH)_6(C_7H_{10}O_6)_6] \cdot (SO_4)_2 \cdot 18H_2O$: C, 23.24; H, 4.89; N, 0.64. Found: C, 23.23; H, 5.05; N, 0.72%.

X-ray Crystal Structure Determination. Single crystals of **1** and **2** were grown from aqueous solutions according to the described synthetic procedures. A single crystal of **1** with dimensions 0.44 × 0.21 × 0.14 mm was mounted on a capillary. A single crystal of **2** with dimensions 0.36 × 0.13 × 0.10 mm was taken directly from the mother liquid and immediately cooled to −113 °C. Diffraction measurements for **1** and **2** were made on a Rigaku R-AXIS SPIDER Image Plate diffractometer using graphite monochromated Mo K_α (for **1**) and Cu K_α (for **2**) radiation. Data collection (ω-scans) and processing (cell refinement, data reduction, and empirical absorption correction) were performed using the CrystalClear program package.[23] Important crystallographic data for both structures are listed in Table 1. Further experimental crystallographic details: for **1**, $2\theta_{max} = 50°$; reflections collected/unique, 33383/16508 [$R_{int} = 0.0289$]/16508; 1115 parameters refined; $\Delta/\sigma = 0.005$; $(\Delta\rho)_{max}/(\Delta\rho)_{min} = 0.575/-1.151$ e/Å^3; R/R_w (for all data), 0.0548/0.1491. For **2**, $2\theta_{max} = 130°$; reflections collected/unique/used, 35313/2392 [$R_{int} = 0.0351$]/2392; 216 parameters refined; $\Delta/\sigma = 0.000$; $(\Delta\rho)_{max}/(\Delta\rho)_{min} = 0.607/-0.509$ e/Å^3; R/R_w (for all data), 0.0494/0.1320.

The structures of **1** and **2** were solved by direct methods using SHELXS-97[24] and refined by full-matrix least-squares techniques on F^2 with SHELXL-97.[25] All hydrogen atoms in **1** and **2** were located by difference maps and were refined isotropically or were introduced at calculated positions as riding on bonded atoms. No hydrogen atoms for the lattice water molecules were included in the refinement. All non-hydrogen atoms in **1** and **2** were refined anisotropically. The lattice water molecules were treated as follows: in **1** there are 52 crystallographically independent sites in the asymmetric unit assigned as oxygen atoms; only 10 of them were refined anisotropically with full occupancy, whereas the rest of them were refined with occupancy factors fixed at less than 0.5 (only four of which were refined anisotropically). In **2**, one of the lattice water molecules was refined anisotropically with full occupancy, and two were found disordered over two positions and refined anisotropically with occupancy factors fixed at 0.5. The rest were refined isotropically with occupancy factors fixed at less than 0.5.

Synthesis. Trinuclear Fe(III)−acetate, $[Fe_3O-(CH_3COO)_6(H_2O)_3] \cdot (NO_3) \cdot 4H_2O$, used as a starting material for the synthesis of **1**, was isolated at very acidic pH in a crystalline form.[22] Its identity was proven through: (a) elemental analysis and FT-IR

Table 1. Summary of Crystal, Intensity Collection, and Refinement Data for $[Fe_7O_3(OH)_3(C_7H_{10}O_6)_6]\cdot20.5\ H_2O$ (1) and $(NH_4)[Fe_7(OH)_6(C_7H_{10}O_6)_6]\cdot(SO_4)_2\cdot18H_2O$ (2)

	1	2
formula	$C_{42}H_{104}Fe_7O_{62.50}$	$C_{42}H_{106}Fe_7NO_{68}S_2$
formula weight	2000.20	2168.35
temperature, K	293 (2)	160 (2)
wavelength	Mo K_a 0.71073	Cu K_a 1.54178
space group	$P2_12_12_1$	$P6_322$
a (Å)	11.1003(2)	16.2964(3)
b (Å)	21.0919(5)	16.2964(3)
c (Å)	40.3401(8)	18.6865(3)
V, (Å^3)	9444.7(3)	4297.8(1)
α (deg)	90.00	90.00
β (deg)	90.00	90.00
γ (deg)	90.00	120.00
Z	4	2
D_{calcd} (Mg m^{-3})	1.407	1.676
abs. coeff. (μ), mm^{-1}	1.144	10.733
range of h,k,l	$-11 \le h \le 13$	$-18 \le h \le 18$
	$-23 \le k \le 25$	$-19 \le k \le 19$
	$-47 \le l \le 47$	$-16 \le l \le 20$
goodness-of-fit on F^2	1.055	1.068
R^a	$R = 0.0490^b$	$R = 0.0446^b$
$R_w{}^a$	$R_w = 0.1435^b$	$R_w = 0.1273^b$

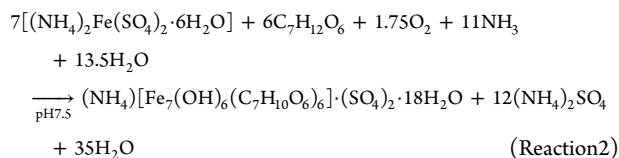$^a R$ values are based on F values, R_w values are based on F^2.

$$R = \frac{\sum \|F_o| - |F_c\|}{\sum (|F_o|)}, \quad R_w = \sqrt{\sum [w(F_o{}^2 - F_c{}^2)^2]/\sum [(wF_o{}^2)^2]}$$

^{b}For 14897 (1) and 2168 (2) reflections with $I > 2\sigma(I)$ $^c w = 1/[\sigma^2(F_o{}^2) + (aP)^2 + bP]$ where $P = (Max\ (F_o{}^2,0) + 2F_c{}^2)/3$

spectroscopy, and (b) X-ray unit cell determination of one of the isolated single crystals of the respective compound. Subsequently, compound **1** was synthesized through a reaction between trinuclear Fe(III) acetate and D-(-)-quinic acid in aqueous media at pH 2.5 and isolated in pure crystalline form. Elemental analyses of the isolated brownish crystalline material suggested a molecular formulation consistent with $[Fe_7O_3(OH)_3(C_7H_{10}O_6)_6]\cdot20.5H_2O$. In this sense, the general stoichiometric reaction leading to the formation of **1** is shown below (Reaction 1):

$$7[Fe_3O(CH_3COO)_6(H_2O)_3]\cdot(NO_3)\cdot4H_2O + 18C_7H_{12}O_6 + 23.5H_2O$$

$$\xrightarrow{pH2.5} 3[Fe_7O_3(OH)_3(C_7H_{10}O_6)_6]\cdot20.5H_2O + 7HNO_3$$

$$+ 42CH_3COOH \qquad \text{(Reaction 1)}$$
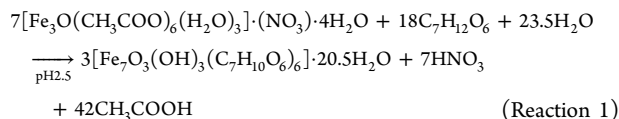
The synthesis of compound **2** was pursued through an expedient synthetic procedure between ferrous iron ions (Mohr's salt) and D-(-)-quinic acid in aqueous media. The pH at which the reaction was run was 7.5 (**2**). Adjustment of pH was achieved through addition of aqueous ammonia, which served as a base, raising the pH of the reaction mixture. Elemental analysis of the isolated crystalline product suggested the molecular formulation $(NH_4)[Fe_7(OH)_6(C_7H_{10}O_6)_6]\cdot(SO_4)_2\cdot18H_2O$ (**2**). The general stoichiometric reaction leading to the formation of compound **2** is shown below (Reaction 2):

$$7[(NH_4)_2Fe(SO_4)_2\cdot6H_2O] + 6C_7H_{12}O_6 + 1.75O_2 + 11NH_3$$

$$+ 13.5H_2O$$

$$\xrightarrow{pH7.5} (NH_4)[Fe_7(OH)_6(C_7H_{10}O_6)_6]\cdot(SO_4)_2\cdot18H_2O + 12(NH_4)_2SO_4$$

$$+ 35H_2O \qquad \text{(Reaction2)}$$

Further confirmation on the structural identity of **1** and **2** came from (a) FT-IR spectroscopy, confirming the presence of quinato

ligands bound to iron ions, and (b) X-ray cell determination of single crystals of each compound (vide infra). Both compounds are soluble in water, but insoluble in organic solvents. They are both stable in the air at room temperature for long periods of time.

X-ray Crystallographic Structures. The X-ray crystal structure of **1** reveals the presence of a discrete seven iron assembly held by six quinato ligands $[C_7H_{10}O_6]^{2-}$ as well as oxido- and hydroxido-bridges in the lattice. The seven-iron assembly is planar with the largest deviation being 0.035 Å for Fe(2). The DIAMOND structure for **1** is shown in Figure 1, and a list of selected bond distances and angles is
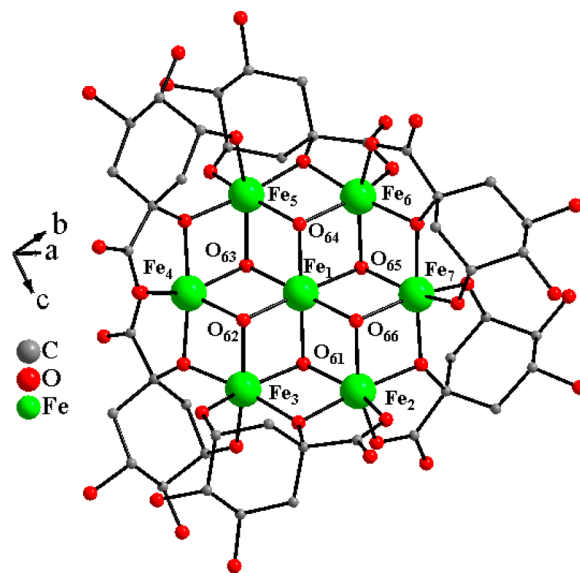
Figure 1. DIAMOND structure of the $[Fe_7(OH)_3(O)_3(C_7H_{10}O_6)_6]$ assembly in **1**, with the atom labeling scheme. Hydrogen atoms have been omitted for clarity.

provided in Table 2 (Supporting Information, Table S1). Compound **1** crystallizes in the orthorhombic space group $P2_12_12_1$ with four molecules per unit cell. Each iron center is six-coordinate, with the geometry being distorted octahedral. Bond valence calculations for all Fe atoms give values in the range 2.81−3.08, indicating a +3 oxidation state for all iron atoms in **1**. This is further supported by Mössbauer spectroscopic studies (Supporting Information, Figure S6A). The central iron Fe(1) is coordinated to six oxygen atoms. Each oxygen acts either as an oxido bridge (O(62), O(64), O(66)) or a hydroxido bridge (O(61), O(63), O(65)), respectively, thereby linking the central iron to the remaining six iron centers (Fe(2)−Fe(7)). The Fe−O_{oxido} and Fe−$O_{hydroxido}$ bond distances are in the range 1.974(3)−2.035(3) and 2.053(3)−2.104(3) Å, respectively. The weakening of Fe−$O_{hydroxido}$ distances with respect to Fe−O_{oxido} are consistent with the assignment of O(62), O(64), O(66) atoms as oxido and those of O(61), O(63), O(65) as hydroxido. The bond valence sum values for the oxido atoms are in the range of 1.20−1.31 and those for hydroxido are in the range 1.44−1.62. All six oxido and hydroxido entities act as triple bridges, thereby generating abutting Fe_2O_2 and $Fe_2O(OH)$ cores. Therefore, six four-membered metallacyclic rings appear in the form $Fe_{central}−(\mu_3−OH)−Fe_{peripheral}−(\mu_3−O)$ with $Fe_{central}\cdots Fe_{peripheral}$ distances in the range of 3.074−3.165 Å. Concurrently, six other peripheral Fe_2O_2 cores emerge from the participation of the deprotonated alkoxido terminal of the quinato ligand in the vicinity of the iron-oxido core(s) with $Fe_{peripheral}\cdots Fe_{peripheral}$ distances in the range 3.061−3.155 Å. The Fe−$O_{alkoxido}$ bond distances are in the range of 1.961(3)−2.001(3) Å. The remaining four coordination sites in those cores are occupied by oxygen atoms provided by adjacently located pairs of deprotonated quinato ligands. In particular, each quinato ligand in **1** is doubly deprotonated and coordinated to two adjacent iron atoms in each core, with the deprotonated sites being: (a) the carboxylato group and (b) the α-alkoxido group. Specifically,

Table 2. Selected Bond Lengths [Å] and Angles [deg] for 1

| distances					
Fe(1)−O(62)	1.974(3)	Fe(3)−O(62)	1.990(3)	Fe(5)−O(34)	2.062(3)
Fe(1)−O(64)	1.976(3)	Fe(3)−O(4)	2.040(3)	Fe(5)−O(63)	2.089(3)
Fe(1)−O(66)	2.022(3)	Fe(3)−O(14)	2.069(3)	Fe(6)−O(41)	1.987(4)
Fe(1)−O(61)	2.090(3)	Fe(3)−O(61)	2.093(3)	Fe(6)−O(31)	1.993(4)
Fe(1)−O(63)	2.094(3)	Fe(4)−O(21)	1.988(4)	Fe(6)−O(32)	2.000(3)
Fe(1)−O(65)	2.104(3)	Fe(4)−O(11)	1.997(4)	Fe(6)−O(42)	2.000(3)
Fe(2)−O(1)	1.983(3)	Fe(4)−O(62)	1.997(3)	Fe(6)−O(64)	2.019(3)
Fe(2)−O(52)	1.989(3)	Fe(4)−O(12)	1.997(3)	Fe(6)−O(65)	2.084(3)
Fe(2)−O(51)	1.992(4)	Fe(4)−O(22)	2.012(3)	Fe(7)−O(52)	1.972(3)
Fe(2)−O(2)	2.001(3)	Fe(4)−O(63)	2.078(3)	Fe(7)−O(42)	1.972(3)
Fe(2)−O(66)	2.035(3)	Fe(5)−O(32)	1.961(3)	Fe(7)−O(44)	2.022(3)
Fe(2)−O(61)	2.053(3)	Fe(5)−O(22)	1.967(3)	Fe(7)−O(54)	2.026(4)
Fe(3)−O(2)	1.973(3)	Fe(5)−O(64)	1.987(3)	Fe(7)−O(66)	2.035(3)
Fe(3)−O(12)	1.974(3)	Fe(5)−O(24)	2.029(3)	Fe(7)−O(65)	2.103(3)
angles					
O(62)−Fe(1)−O(61)	81.6(1)	Fe(2)−O(61)−Fe(1)	98.1(1)	Fe(6)−O(65)−Fe(7)	97.8(1)
O(66)−Fe(1)−O(61)	80.2(1)	Fe(2)−O(61)−Fe(3)	98.5(1)	Fe(6)−O(65)−Fe(1)	95.1(1)
O(62)−Fe(1)−O(63)	81.9(1)	Fe(1)−O(61)−Fe(3)	95.0(1)	Fe(7)−O(65)−Fe(1)	97.6(1)
O(64)−Fe(1)−O(63)	80.1(1)	Fe(1)−O(62)−Fe(3)	102.2(1)	Fe(1)−O(66)−Fe(7)	102.6(1)
O(64)−Fe(1)−O(65)	82.0(1)	Fe(1)−O(62)−Fe(4)	101.4(1)	Fe(1)−O(66)−Fe(2)	100.9(1)
O(66)−Fe(1)−O(65)	80.0(1)	Fe(3)−O(62)−Fe(4)	100.3(1)	Fe(7)−O(66)−Fe(2)	99.2(1)
O(66)−Fe(2)−O(61)	80.7(1)	Fe(4)−O(63)−Fe(5)	97.8(2)	Fe(7)−O(42)−Fe(6)	105.2(2)
O(62)−Fe(3)−O(61)	81.2(1)	Fe(4)−O(63)−Fe(1)	94.9(1)	Fe(3)−O(2)−Fe(2)	104.4(2)
O(62)−Fe(4)−O(63)	81.7(1)	Fe(5)−O(63)−Fe(1)	96.2(1)	Fe(5)−O(22)−Fe(4)	104.2(1)
O(64)−Fe(5)−O(63)	80.0(1)	Fe(1)−O(64)−Fe(5)	103.6(2)	Fe(5)−O(32)−Fe(6)	101.3(2)
O(64)−Fe(6)−O(65)	81.5(1)	Fe(1)−O(64)−Fe(6)	101.4(2)	Fe(5)−O(64)−Fe(6)	99.7(1)
O(66)−Fe(7)−O(65)	79.7(1)				
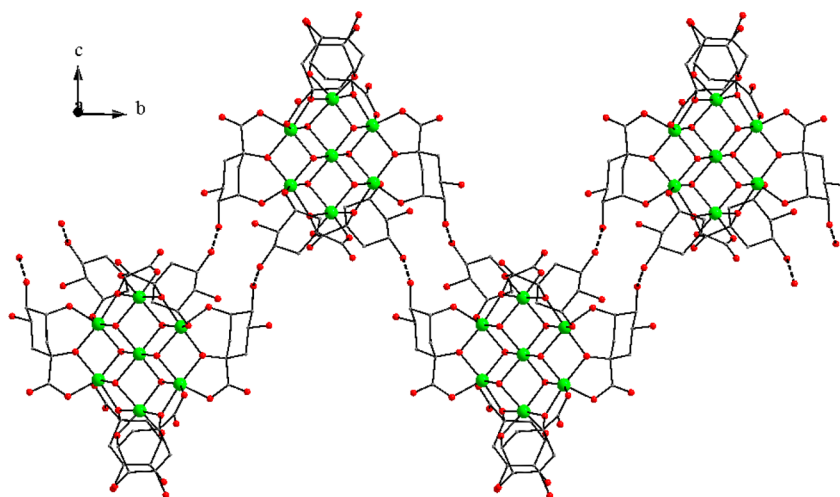
Figure 2. Small segment of the helical chains in the structure of **1** due to hydrogen bonds (dashed lines).

the mode of coordination of each quinato ligand projects binding of the α-hydroxycarboxylic acid moiety to one iron center, with the first alcoholic moiety spanning over and binding to the second iron center. The alcoholic moiety of each quinato ligand bound to the iron center in every dinuclear unit remains protonated with bond distances in the range of 2.022(3)−2.040(3) Å. The Fe−O$_{carboxylato}$ bond distances are in the narrow range of 1.983(3)−1.997(4) Å. The second carboxylato oxygen and the other two alcoholic groups of all six quinato ligands are not bound to iron centers and thus stand away from the actual Fe$_7$ core assembly. To this end, five-membered metallacyclic rings form through the carboxylato and α-hydroxido oxygens, while six-membered metallacyclic rings arise through the α-hydroxido and alcoholato oxygens, thereby rendering the arising dinuclear units and the Fe$_7$ species quite stable. Consequently, three of the six iron centers

(Fe(2), Fe(4), Fe(6)) in **1** have their four remaining coordination sites occupied through formation of two five-membered metallacyclic rings formed by two adjacently located quinic acids. The three remaining iron centers (Fe(3), Fe(5), Fe(7)) fulfill their octahedral coordination site requirements through formation of two six-membered metallacyclic rings formed by two adjacently located quinic acids.

The heptanuclear clusters are held together through strong intermolecular hydrogen bonds [O6···O45 (2 − x, −0.5 + y, 0.5 − z) = 2.765 Å, H6O···O45 = 2.062 Å, O6−H6O···O45 = 143.7 °; O56···O15 (2 − x, 0.5 + y, 0.5 − z) = 2.712 Å, H56O···O15 = 1.917 Å, O56−H56O···O15 = 162.9 °], thus forming helical chains parallel to the b axis; the pitch of the helix calculated as the Fe$_{central}$···Fe$_{central}$ interatomic distance is 15.172 Å, and the angle between the mean planes of adjacent Fe$_7$ entities is 65.42 ° (Figure 2). These helices are

further linked through water molecules of crystallization, which are present in the lattice of **1**, thereby generating an overall 3D network of hydrogen bonds bestowing substantial stability in the arisen crystal lattice (Supporting Information, Table S2).

The X-ray crystal structure of **2** reveals the presence of discrete seven-iron assemblies held by six quinato ligands $[C_7H_{10}O_6]^{2-}$ and six hydroxido-bridges. Moreover, sulfate and ammonium ions are present in the lattice of **2**. The DIAMOND structure for the cationic assembly $[Fe_7(OH)_6(C_7H_{10}O_6)_6]^{3+}$ in **2** is shown in Figure 3. A list of selected
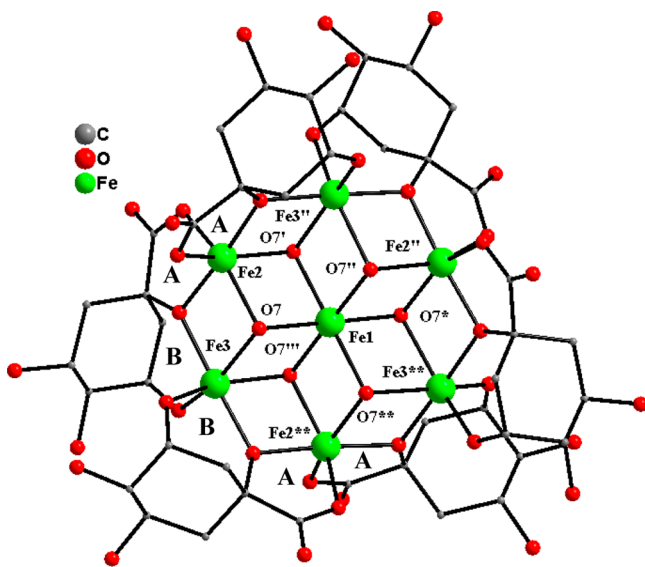

Figure 3. DIAMOND structure of the cationic assembly $[Fe_7(OH)_6(C_7H_{10}O_6)_6]^{3+}$ in **2**, with the atom labeling scheme. (A) indicates the five-membered and (B) the six membered metallacyclic rings in the heptanuclear core. Hydrogen atoms have been omitted for clarity. Primed atoms are generated by symmetry: (') $1 - y$, $1 - x$, $0.5 - z$; (") $-x + y$, $1 - x$, z; (''') x, $1 + x - y$, $0.5 - z$; (*) $-x + y$, y, $0.5 - z$, (**) $1 - y$, $1 + x - y$, z.

bond distances and angles for **2** is given in Table 3. Compound **2** crystallizes in the hexagonal crystal system and in the space group $P6_322$, with two molecules per unit cell. Fe(1) occupies the 2c Wyckoff position, which possesses 3.2 symmetry (the 2-fold axes are parallel to the tertiary directions of the hexagonal cell which pass through the (0,0,1/4) point). Fe(2) and Fe(3) lie on the aforementioned axes (occupy 6h Wyckoff positions) and as a consequence the whole Fe_7 entity is strictly planar. Bond valence calculations for the three symmetry independent iron atoms give values close to 3, indicating a +3 oxidation state for all iron atoms in **2**. This is further supported by Mössbauer spectroscopic studies (Supporting Information, Figure S6B). The sulfate anion also sits on the same 3-fold axis, which passes through the sulfur and O(11) atom; the sulfate anion is capping the Fe_7 plane at a distance of 4.148 Å (for S) and 3.664 Å (for O(12)). Every iron center in **2** is six coordinate, with the geometry being distorted octahedral. The central iron atom (Fe(1)) is coordinated to six oxygen atoms that act as triply bridging hydroxido moieties (O(7)) with bond distances at 2.057(3) Å. They each coordinate to the central iron in a way that six internal four-membered metallacyclic rings arise forming $Fe(1)_{central}-(\mu_3-OH)-Fe_{peripheral}-(\mu_3-OH)$ cores with $Fe_{central}\cdots Fe_{peripheral}$ distances in the range of 3.147–3.234 Å and $Fe_{peripheral}-O_{hydroxido}$ bond distances at 2.070(3) and 2.144(3) Å for Fe(2)−O(7) and Fe(3)−O(7), respectively. These bond distance values indicate a weakening of Fe(III) bonds with hydroxido oxygen atoms, a fact which is reflected in the values of the bond valence sum calculated for O(7), which is 1.23, and is consistent with the assignment of these oxygen atoms as hydroxido entities. All six coordination sites around the iron centers are occupied by the triply bound hydroxido bridge oxygens. Concurrently, six other peripheral $Fe(1)-(\mu_3-OH)-Fe-(\mu_2-O)$ cores emerge from the participation of the deprotonated alkoxido terminal of the quinato ligand in the vicinity of the iron−hydroxido core(s) with $Fe_{peripheral}\cdots Fe_{peripheral}$ distances at ≈3.19 Å. The Fe−O$_{alkoxido}$ bond distances are 1.974(3) and 1.997(3) Å to Fe(2) and Fe(3), respectively. The remaining four coordination sites in those external cores are occupied by oxygen atoms provided by adjacently located pairs of deprotonated quinato ligands. In particular, each quinato ligand is doubly deprotonated and coordinated to two adjacent iron atoms in each core, with the deprotonated sites being (a) the carboxylato group and (b) the α-alkoxido group. Specifically, the

Table 3. Selected Bond Lengths [Å] and Angles [deg] for 2

distances					
Fe(1)−O(7')	2.057(3)	Fe(2)−O(2")	1.974(3)	Fe(3)−O(4''')	1.987(3)
Fe(1)−O(7)	2.057(3)	Fe(2)−O(2''')	1.974(3)	Fe(3)−O(4)	1.987(3)
Fe(1)−O(7")	2.057(3)	Fe(2)−O(1")	1.979(3)	Fe(3)−O(2''')	1.997(3)
Fe(1)−O(7''')	2.057(3)	Fe(2)−O(1''')	1.979(3)	Fe(3)−O(2)	1.997(3)
Fe(1)−O(7*)	2.057(3)	Fe(2)−O(7)	2.070(3)	Fe(3)−O(7)	2.144(3)
Fe(1)−O(7**)	2.057(3)	Fe(2)−O(7')	2.070(3)	Fe(3)−O(7''')	2.144(3)
angles					
O(7')−Fe(1)−O(7)	80.9(2)	O(2")−Fe(2)−O(2''')	176.2(2)	O(4''')−Fe(3)−O(4)	106.0(2)
O(7')−Fe(1)−O(7")	81.4(2)	O(2")−Fe(2)−O(1")	80.2(1)	O(4''')−Fe(3)−O(2''')	88.0(1)
O(7)−Fe(1)−O(7")	98.9(1)	O(2''')−Fe(2)−O(1")	97.5(1)	O(4)−Fe(3)−O(2''')	93.2(1)
O(7')−Fe(1)−O(7''')	98.9(1)	O(2")−Fe(2)−O(1''')	97.5(1)	O(4''')−Fe(3)−O(2)	93.2(1)
O(7)−Fe(1)−O(7''')	81.4(2)	O(2''')−Fe(2)−O(1''')	80.2(1)	O(4)−Fe(3)−O(2)	88.0(1)
O(7")−Fe(1)−O(7''')	179.7(2)	O(1")−Fe(2)−O(1''')	103.8(2)	O(2''')−Fe(3)−O(2)	178.1(2)
O(7')−Fe(1)−O(7*)	98.9(1)	O(2")−Fe(2)−O(7)	104.8(1)	O(4''')−Fe(3)−O(7)	157.3(1)
O(7)−Fe(1)−O(7*)	179.7(2)	O(2''')−Fe(2)−O(7)	78.2(1)	O(4)−Fe(3)−O(7)	91.0(1)
O(7")−Fe(1)−O(7*)	80.9(2)	O(1")−Fe(2)−O(7)	92.4(1)	O(2''')−Fe(3)−O(7)	75.9(1)
O(7''')−Fe(1)−O(7*)	98.9(1)	O(1''')−Fe(2)−O(7)	154.4(1)	O(2)−Fe(3)−O(7)	102.5(1)
O(7')−Fe(1)−O(7**)	179.7(2)	O(2")−Fe(2)−O(7')	78.2(1)	O(4''')−Fe(3)−O(7''')	91.0(1)
O(7)−Fe(1)−O(7**)	98.9(1)	O(2''')−Fe(2)−O(7')	104.8(1)	O(4)−Fe(3)−O(7''')	157.3(1)
O(7")−Fe(1)−O(7**)	98.9(1)	O(1")−Fe(2)−O(7')	154.4(1)	O(2''')−Fe(3)−O(7''')	102.5(1)
O(7''')−Fe(1)−O(7**)	80.9(2)	O(1''')−Fe(2)−O(7')	92.4(1)	O(2)−Fe(3)−O(7''')	75.9(1)
O(7*)−Fe(1)−O(7**)	81.4(2)	O(7)−Fe(2)−O(7')	80.3(2)	O(7)−Fe(3)−O(7''')	77.4(2)

^{a}Symmetry operations: (') $1 - y$, $1 - x$, $0.5 - z$; (") $-x + y$, $1 - x$, z; (''') x, $x - y + 1$, $0.5 - z$; (*) $-x + y$, y, $0.5 - z$; (**) $1 - y$, $x - y + 1$, z.
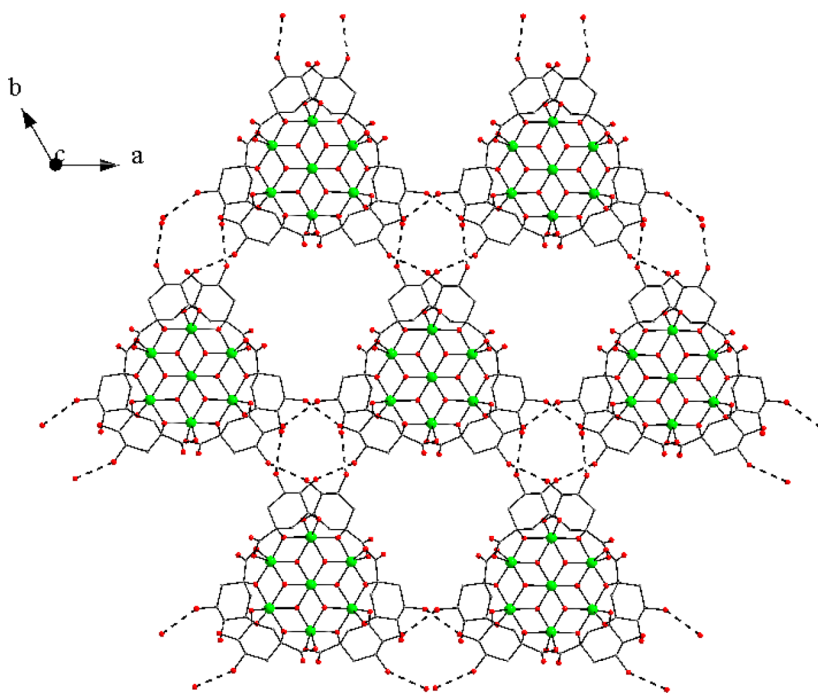
Figure 4. Small fragment of the 2D network in the structure of **2** due to hydrogen bonds (dashed lines).

mode of coordination of each quinato ligand projects binding of the α-hydroxycarboxylic acid moiety to one iron center, with the first terminal alcoholic moiety spanning over and binding to the second iron center. The alcoholic moiety of each quinato ligand bound to iron center in every dinuclear unit remains protonated with distances at 1.987(3) Å. The Fe−O$_{carboxylato}$ bond distances are 1.979(3) Å. The second carboxylato oxygen and the other two alcoholic groups of all six quinato ligands refrain from binding, thereby dangling away from the actual Fe$_7$ core assembly. The total number of quinato binders bound to the Fe$_7$ assembly is six. Three Fe(III) ions (Fe(2)) in **2** have the same coordination environment with (a) two coordination sites occupied by two triply bridging hydroxido moieties (O(7)) and (b) the other four coordination sites being occupied by two abutting quinic acids promoting formation of two discrete five-membered metallacyclic rings of the type O(2)−C(2)−C(1)−O(1)−Fe(2) (Figure 3). Finally, the remaining three Fe(III) ions (Fe(3)) present in the lattice of **2** have the same coordination environment yet different from that of the aforementioned three iron ions (Fe(2)). In particular, two of the six coordination sites are occupied by two hydroxido bridges (O(7)), while the other four sites are taken up by two quinic acids forming two discrete six-membered metallacyclic rings of the type O(2)−C(2)−C(3)−C(4)−O(4)−Fe(3) (Figure 3). The positive charge of the heptanuclear iron core is counteracted by the presence of two sulfate ions. An additional ammonium counterion and 18 molecules of water of crystallization are present in the lattice of **2**.

The heptanuclear cations are held together through hydrogen bonds [O6⋯O5 (−1 − x + y, −x, z) = 3.020 Å, H6O⋯O5 = 2.460 Å, O6−H6O⋯O5 = 125.0 °], thus creating a 2D network which extends parallel to the *ab* plane (Figure 4). The sulfate and ammonium counterions as well as the water molecules of crystallization are also involved in hydrogen bonding interactions, thus generating an overall 3D framework in the lattice of **2** (Supporting Information, Table S3).

Variable coordination modes of numerous carboxylate-bearing ligands were previously observed, leading to the formation of heptanuclear Fe(III) species. The Fe−O distances are in the range from 1.961(3) to 2.104(3) Å found in **1** and in the range from 1.974(3) to 2.144(3) Å found in **2**. Examples of heptanuclear Fe(III) complexes include the following species: [Fe$^{III}_7$(μ_3−O)$_3$(teaH)$_3$(μ−O$_2$CCMe$_3$)$_6$(η^1−O$_2$CCMe$_3$)$_3$(H$_2$O)$_3$] (1.892(2)−2.002(2) Å) (**3**),[26] [Fe$^{III}_7$(μ_3−O)$_3$(bdea)$_3$(μ−O$_2$CCMe$_3$)$_6$(η^1−O$_2$CCMe$_3$)$_3$(H$_2$O)$_3$]

(1.856(2)−2.011(2) Å) (**4**),[26] [Fe$^{III}_7$(μ_3−O)$_3$(phdeaH)$_3$(μ−O$_2$CCMe$_3$)$_6$(η^1−O$_2$CCMe$_3$)$_3$(H$_2$O)$_3$] (1.866(2)−2.003(2) Å) (**5**)[26] where teaH$_3$ = triethanolamine, bdeaH$_2$=*N*-butyldiethanolamine and phdea = phenyldiethanolamine, respectively, [Fe$^{III}_7$O$_3$(O$_2$CCMe$_3$)$_9$(bheapH)$_3$(H$_2$O)$_3$] (1.852(5)−2.102(5) Å) (**6**),[27] [Fe$^{III}_7$O$_3$(O$_2$CCMe$_3$)$_9$(teaH)$_3$(H$_2$O)$_3$] (1.852(6)−2.110(6) Å) (**7**),[27] where bheapH$_3$ = 1-[*N,N*-bis(2-hydroxyethyl)-amino]-2-propanol. Heptanuclear mixed Fe(II,III) species have been reported, including [Fe^{III}Fe$^{II}_6$(MeO)$_6$(HL)$_6$]Cl$_3$ (2.041(3)−2.367(4) Å) (**8**),[28] where H$_2$L = 3-methoxy-2-salicylideneamino-1-ethanol, and [Fe^{II}Fe$^{III}_6$(tea)$_6$](ClO$_4$)$_2$ (2.123(3)−2.181(4) Å) (**9**),[29] and [Fe$^{II}_3$Fe$^{III}_4$(C$_4$H$_9$NO$_2$)$_6$Cl$_6$]·2CH$_3$CN·H$_2$O (1.994(5)−2.203(5) Å) (**10**).[30]

The quinato ligand plays the role of an efficient metal ion chelator (mode I and mode II in Scheme 1), capable of effectively formulating

Scheme 1
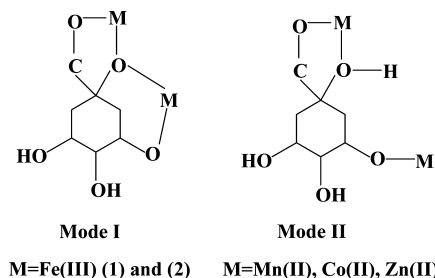
the coordination environment around iron ions in **1** and **2**. This coordination ability has also been observed in the case of (di-, multi)valent transition metal ions, with representative examples being K[Co(C$_7$H$_{11}$O$_6$)$_3$]·3CH$_3$CH$_2$OH (**11**),[31] [Co(C$_7$H$_{11}$O$_6$)$_2$(H$_2$O)$_2$]·3H$_2$O (**12**),[31] Na[Ni(C$_7$H$_{11}$O$_6$)$_3$]·2.75H$_2$O (**13**),[32] {[Cu(C$_7$H$_{10}$O$_6$)(H$_2$O)]$_2$(H$_2$O)}$_2$ (**14**),[33] {[CuCl(C$_7$H$_{11}$O$_6$)(H$_2$O)]·H$_2$O}$_n$ (**15**),[34] [Zn(C$_7$H$_{11}$O$_6$)$_2$] (**16**),[35] [Cd(C$_7$H$_{11}$O$_6$)$_2$]·H$_2$O (**17**),[35] [Co$_2$(C$_7$H$_{11}$O$_6$)$_4$]$_n$·nH$_2$O·(**18**),[36] [Zn$_3$(C$_7$H$_{11}$O$_6$)$_6$]$_n$·nH$_2$O (**19**),[36] and [Pt(C$_6$H$_{14}$N$_2$)(C$_7$H$_{10}$O$_6$)] (**20**).[37] Only three mononuclear Fe(III)−quinato species have been reported: (Cat)[Fe(C$_7$H$_{11}$O$_6$)$_3$]·

(OH)·yH$_2$O where (Cat)/y = NH$_4^+$/0 (**21**), K$^+$/3 (**22**), Na$^+$/8 (**23**), respectively.[38]

The angles were in the range of 77.6(1)−107.5(1) ° for **1** and 75.9(1)−106.0(1) ° for **2**, respectively, and hence varied broadly around the ideal octahedral angle of 90°. The aforementioned angle values were similar to those observed in **3**−**10**. Moreover, the angles were similar to the ones in the three mononuclear Fe(III)−quinate species: 78.08(7)−105.23(8) ° (**21**), 78.51(1)−104.91(1) ° (**22**), 79.10(2)−106.46(2) ° (**23**).

Electronic Spectroscopy. The UV−vis spectra of **1** and **2** were recorded in H$_2$O (Supporting Information, Figures S1 and S2). The spectra showed a band at λ_{max} = 316 nm ($\varepsilon \sim$18620 M^{-1} cm^{-1}) for **1** and λ_{max} = 325 nm ($\varepsilon \sim$ 6089 M^{-1} cm^{-1}) for **2**, respectively, with the latter feature rising well into the ultraviolet region. Both bands have been attributed to the presence of a quinato oxygen to Fe(III) Ligand to Metal Charge Transfer (LMCT). The spectra were featureless beyond 400 nm.

Infrared Spectroscopy. The FT-IR spectra of **1** and **2** in KBr exhibit strong absorptions for the carbonyl carboxylato groups in both the antisymmetric and symmetric vibration regions. The antisymmetric stretching vibrations ν_{as}(COO$^-$) appear in the range from 1623 to 1584 cm^{-1} (**1**) and around 1628 cm^{-1} (**2**), whereas the corresponding symmetric stretches ν_s(COO$^-$) appear in the range from 1429 to 1381 cm^{-1} (**1**) and around 1404 cm^{-1} (**2**). The frequencies for the carbonyl stretches in **1** and **2** are shifted to lower values in comparison to those of free D-(-)-quinic acid, indicating changes in the vibrational status of the ligand upon coordination to the metal ion.[39]

Thermal Studies. The thermal decomposition of both **1** and **2** was studied by TGA-DTG under an atmosphere of oxygen (Supporting Information, Figures S3 and S4). The TGA diagram shows an initial process reaching a temperature of 235 °C, involving loss of water molecules in **1**. The observed total weight loss of water amounts to 44%, a value close to the calculated value of 46% based on the molecular formula of **1**. Additional steps are observed in the ensuing thermal process up to 470 °C, corresponding to the decomposition of the organic moiety bound to Fe(III). Beyond that temperature, a stable line is observed consistent with the formation of Fe$_2$O$_3$, amounting to ∼28% in very good agreement with the calculated value of 28% based on the molecular formula of **1**. The stable behavior on the thermal decomposition of **1** extends out to 800 °C.

In much the same fashion, the TGA diagram of **2** shows an initial process reflecting the loss of water molecules. The release of all water molecules up until ∼251 °C corresponds to an observed weight loss of 43%. Additional steps are observed owing to the decomposition of the organic moiety in **2**. The total weight loss due to the decomposition of the organic composition of **2** is 45.7% and is reached at approximately 935 °C, signifying an endothermic process.

Cyclic Voltammetry. The cyclic voltammetry of **1** and **2** was studied in aqueous solutions in the presence of KNO$_3$ as a supporting electrolyte. The cyclic voltammogram of both compounds projects an ill-defined electrochemical behavior with an irreversible wave at E_{pc} = −0.70 V (**1**) and E_{pc} = −0.72 V (**2**) versus Ag/AgCl, respectively. The irreversible reduction wave likely reflects complex process(es) involving the Fe(III)/Fe(II) redox couple in **1** and **2**, with concurrent coordination sphere changes. Attempts to pursue the redox chemistry of **1** and **2** at low reduction potentials are currently ongoing.

Magnetic Susceptibility Studies. The temperature dependence of $\chi_M T$ (χ_M being the magnetic susceptibility for seven Fe(III) ions) for complex **1** (solid stars) and **2** (open stars) is shown in Figure 5. The $\chi_M T$ value is 19.35/17.55 cm^3 mol^{-1} K at 300 K, significantly lower than the value expected for seven isolated ions of Fe(III), which is 7 × 4.38 cm^3 mol^{-1} K. From 300 K down to 10 K, there is a smooth linear decrease, while below that temperature and toward 2 K, a more pronounced decrease is observed, reaching the value of 2.0 cm^3 mol^{-1} K for both compounds. In order to avoid overparameterization, the same magnetic model was used to fit the susceptibility data of **1** and **2** assuming a 3-fold symmetry. Although in the case of **1**, there is a slight deviation from this symmetry, influencing the exchange integrals, the effects are expected to be weak. On the other hand, the available data do not allow determination of many strong exchange constants
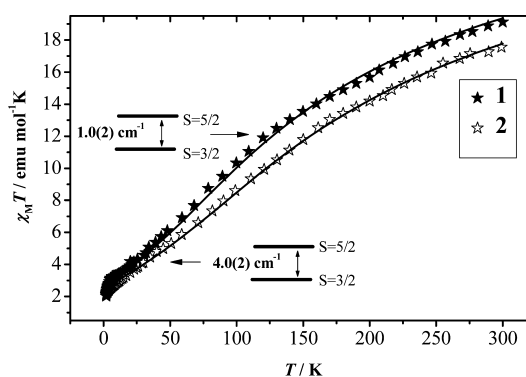
Figure 5. Temperature dependence of the magnetic susceptibility of **1** (solid stars) and **2** (open stars), in the form of $\chi_M T$ vs T, in the temperature range of 2.0−300 K using an external magnetic field of 0.5 T. Solid line represents the fitting results (see text).

because the temperature dependence of χT reflects just a few low-lying spin states. Hence, the simplified magnetic model is described in

Scheme 2
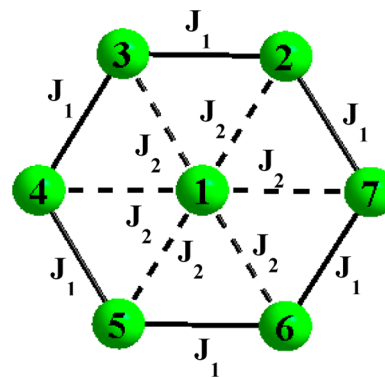
Scheme 2 and is given in eq 1. The susceptibility data were fitted by the following zero-field Hamiltonian:

$$H = -2J_1 \left(\sum_{i=2}^{6} \hat{S}_i \cdot \hat{S}_{i+1} + \hat{S}_7 \cdot \hat{S}_2 \right) - 2J_2 (\hat{S}_2 + \hat{S}_3 + \hat{S}_4 + \hat{S}_5 + \hat{S}_6 + \hat{S}_7) \cdot \hat{S}_1 \quad (1)$$

It was possible to apply the well-known ITO method, where the total dimension of the energy matrix (279936 × 279936) can be reduced (point symmetry reasons) to S-block matrixes, with the maximum size being (3150 × 3150).[40] The best fits for **1** and **2** (solid lines in Figure 5) are given by the following parameters J_1 = −8.8(2)/−7.4(2) cm^{-1}, J_2 = −2.3(2)/1.6(2) cm^{-1} and g = 1.98(1)/1.98(1).

Focusing on diferric complexes, Gorun and Lippard had previously reported an exponential relationship between the exchange constant and a parameter related to the Fe−O distances in oxido-bridged complexes.[41] The Fe−O−Fe angle was found to have only a second-order effect.[42] Weihe and Güdel[43] used a formulation based on the angular overlap model (AOM) to derive an expression for J as a function of both the Fe−O−Fe angle (φ) and the Fe−O distance (r).

Despite the extensive literature devoted to magnetostructural correlations in dinuclear iron(III) compounds, very little has been reported on polynuclear complexes. The exchange becomes more strongly antiferromagnetic (i.e., J has a larger negative value) as the Fe−O distance decreases and the Fe−O−Fe angle increases. This behavior has been noted by Cañada-Vilalta et al.,[44] where it can be seen that the angular dependence is accentuated as r decreases, with the radial dependence being more important at wider angles. While the
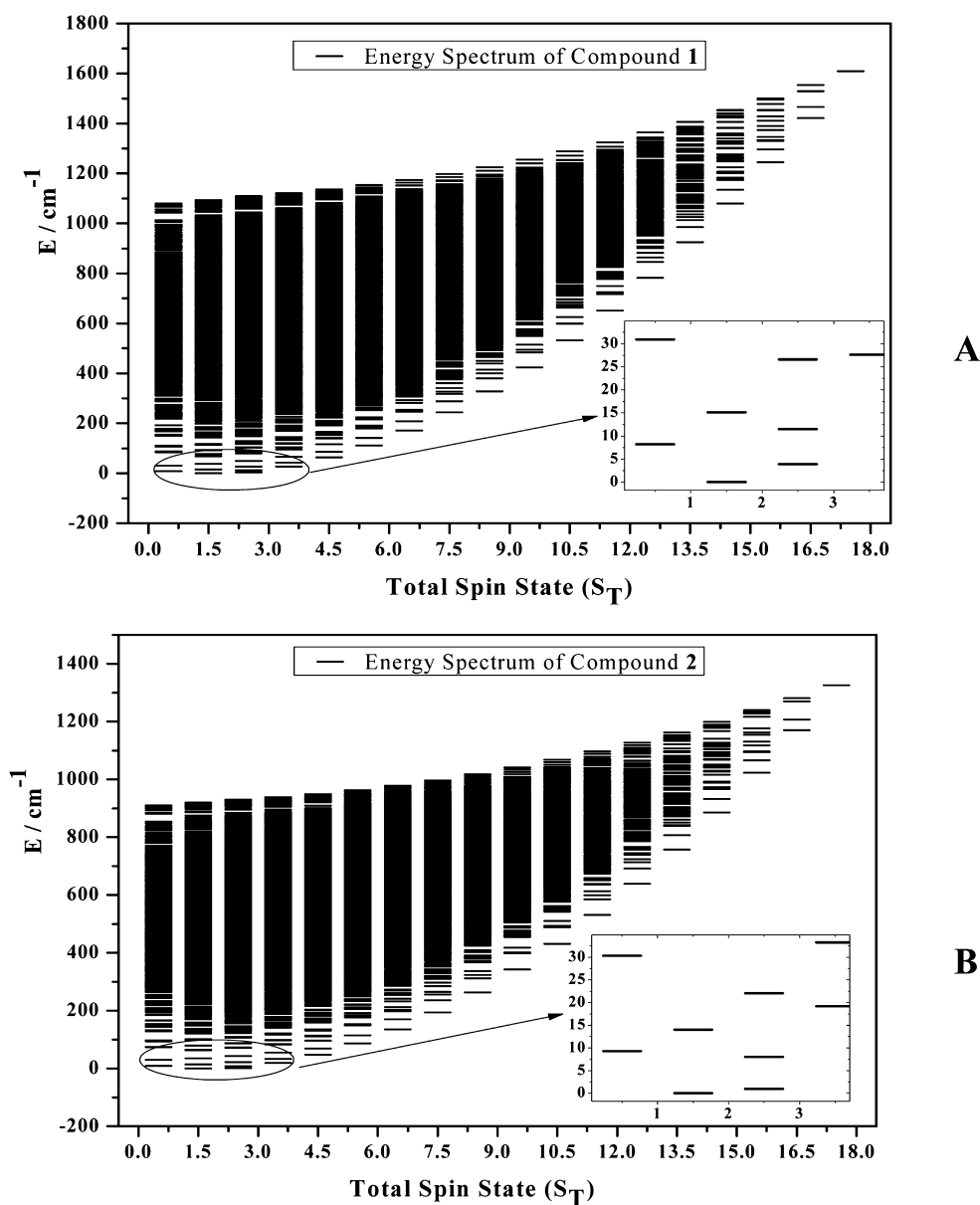
Figure 6. Full energy spectrum of compound **1** (A) and **2** (B) along with a more detailed view of the low lying states.

observation of a radial dependence was expected and is in accord with previous studies on dinuclear Fe(III) compounds, the strong angular dependence is surprising and unprecedented. We believe that this is the case for the small exchange interaction values for both complexes since the Fe−O values are very high. Especially in the case of **2**, the J_2 interaction involves Fe(III) ions with an Fe−O distance of around 2.05 Å, which is the upper limit. A careful inspection of literature data[44] also shows that the values obtained in this work are of the same magnitude. In this sense, it may be that the value of J_2 in complex **2** is overestimated, but still denotes the trend of a very small antiferromagnetic interaction, which probably—due to the topology of spins (triangles)—could yield frustration effects.

According to these values, the ground state is $S = 3/2$ for both **1** and **2**, while the first excited state is an $S = 5/2$, standing 4.0(1)/1.0(1) cm^{-1} higher (Figure 6). These are the first examples of heptanuclear Fe(III) complexes with an $S = 3/2$ ground state, since usually the ground state of antiferromagnetically coupled rings of this type is an $S = 5/2$.[26,27] In order to rationalize our findings, a theoretical calculation of the energy function based on eq 1 was carried out and is shown in eq 2, where the spin-coupling scheme is $S_R = S_2 + S_3 + S_4 + S_5 + S_6 + S_7$ and $S = S_R + S_1$. The first part of this equation was calculated

numerically using the ITO method[45] and corresponds to the interactions of the peripheral Fe(III) ions (α is an additional quantum number for labeling of the different spin levels with the same S_R value as mentioned above).[46] The second part is a simple interpretation of Kambe's method[47] describing the interaction of the central Fe(III) ion with the outer ones. The energy function is the following:

$$E(S, S_R, a) = -2J_1 E_R(S_R, \alpha) - J_2[S(S + 1) - S_R(S_R + 1) - S_7(S_7 + 1)] \tag{2}$$

In Figure S5 (Supporting Information), the total spin of the ground state based on eq 2 as a function of the term $J_2/|J_1|$ (where J_1 was assumed to be antiferromagnetic) is given. For the specific case, the values $J_2/|J_1|$ are −0.26/−0.22, pointing to a ground state of $S = 3/2$ (inset of Figure S5).[26]

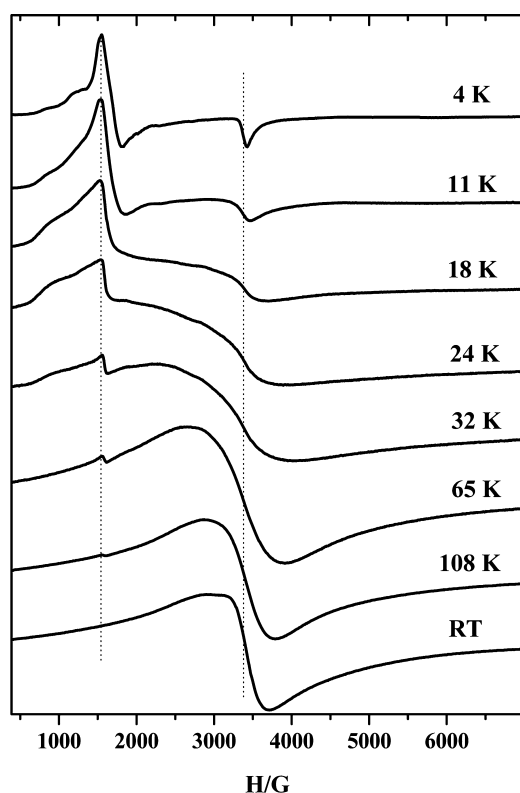Isothermal magnetization curves at $T = 2$ K in an applied field range of 0−5 T are shown in Figure 7 for complex **1** (solid stars) and **2** (open stars). It must be pointed out that in both cases there is a clear contribution of the excited ($S = 5/2$) state to the ground ($S = 3/2$) state, in view of the fact that the magnetization curve exhibits a linear increase at high magnetic fields with no saturation values.
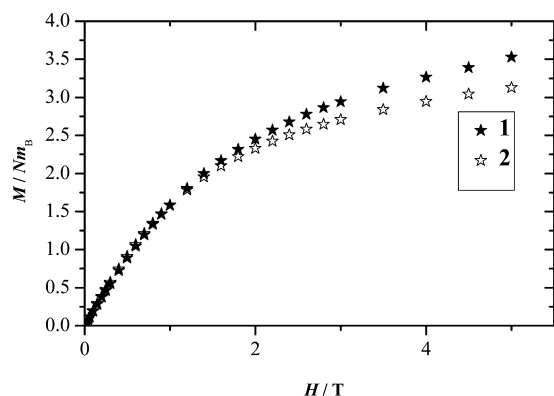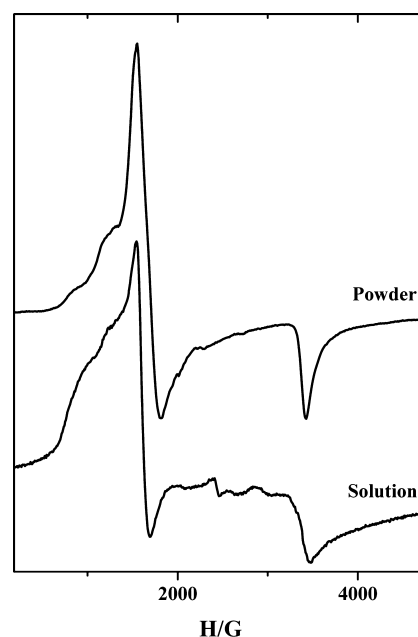
Figure 7. Magnetization of **1** (solid stars) and **2** (open stars), in the form of $M/N\mu_B$ vs H/T, at 2 K and in the field range 0−5 T.

EPR Spectroscopy. X-Band EPR measurements of **1** and **2** were carried out in powder samples as well as in frozen solutions in water and are shown in Figures 8 and 9 for **1** and Figures 10 and 11 for **2**,
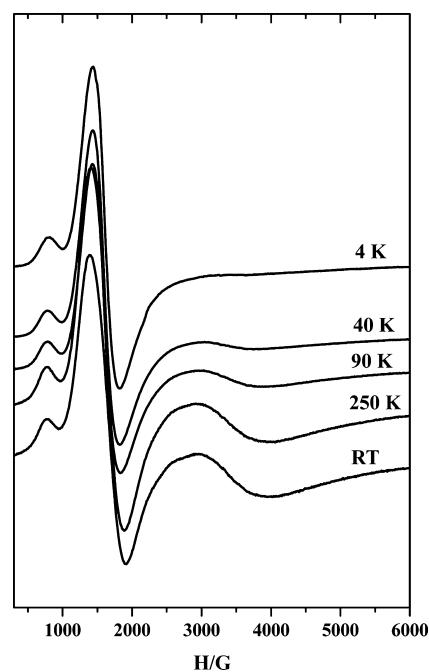

Figure 9. Powder X-Band EPR spectrum and frozen water solution X-Band EPR spectrum of **1** in the field range of 0−5000 G, recorded at 4.2 K.

Figure 8. Temperature dependence of the powder X-band EPR spectrum of **1** in the field range of 0−6000 G.

Figure 10. Temperature dependence of the powder X-band EPR spectrum of **2** in the field range of 0−6000 G.

respectively. The systems retain their structure in solution, where a typical rhombic signal appears at low magnetic fields with prominent features at ≈1000 and 1600 G for both compounds (Figure 9 and 11, respectively). The EPR spectra of finely ground polycrystalline powders of **1** and **2** exhibited similar features and temperature dependences over the range of 295 K down to 2.5 K, although there were some differences in detail as shown in Figure 8 (**1**) and Figure 10 (**2**). A single isotropic broad line at $g \sim 2.0$ and peak-to peak derivative width ~600 G was observed at 295 K for both complexes, while for complex **2**, a second strong rhombic signal appears with prominent features at ≈1000 and 1600 G. As the temperature decreases, the resonance intensity of the central $g \sim 2$ signal decreases. Below 100 K, signals with narrower resonances could be discerned at lower magnetic

fields in the case of **1** that become better resolved as the temperature decreases toward 30 K and below, while in the case of **2** no new signal emerges. The $g \sim 2$ resonance could be observed also at 2 K for **1**, while it disappeared in the case of **2**. The broad resonance observed at and below 295 K is attributed to resonances within the combined spin manifold of the seven Fe(III) ions. As shown by the magnetic susceptibility measurements, only some of the expected states are populated even at 295 K, and even those are swiftly depopulated as temperature decreases. Transitions between the spin levels within the multiplicity of spin states arising from the interactions of the spins of the individual ions are not observed, as they will be averaged out by the fluctuations of the direction of magnetization of the seven Fe(III)
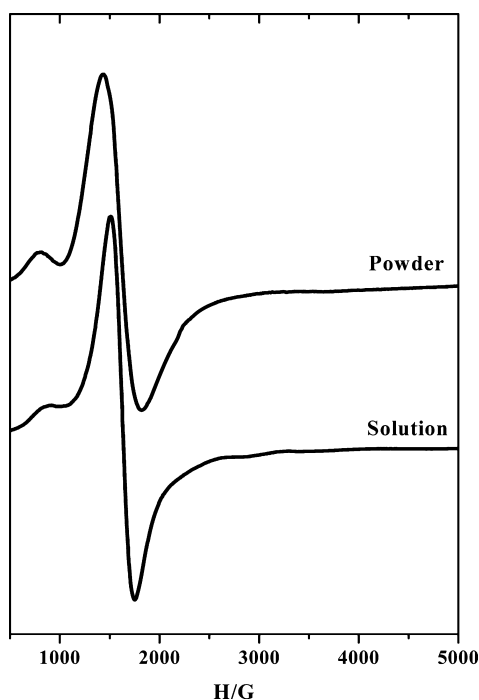
Figure 11. Powder X-Band EPR spectrum of **2** in the field range of 0−5000 G. Frozen water solution X-Band EPR spectrum in the field range of 0−5000 G, recorded at 4.2 K.

cluster. Thus, the resonance arises from dipolar interactions between the seven Fe(III) ions, mediated by what may be described as a process of exchange narrowing. The temperature dependence of this resonance is then readily explained by the depopulation of the higher spin states and the decrease in the dipolar broadening effects as that depopulation takes place. An $S = 3/2$ state is populated at 4 K for both complexes, with $g_{xy} = 4.0$ and $g_z = 2$ for **1**, whereas for **2** only the $g = 4$ is resolved. Also, additional features appear at lower magnetic fields for both compounds denoting population of the excited $S = 5/2$ state even at 4 K, which has been already suggested from the magnetization measurements.

■ DISCUSSION

Structural Diversity in Iron−Quinato Chemistry. The synthesis of the first heptanuclear compounds **1** and **2** between Fe(III) and D-(-)-quinic acid exemplifies the affinity of the aforementioned hydroxylcarboxylate binder toward transition metal ions, such as Fe(III). Undoubtedly, the nature of the iron reagent used to synthesize **1** and **2** was crucial in promoting the investigated reactions and ultimately leading to the isolation of discrete crystalline products in a suitable form for further characterization. Compound **1** arose from a trinuclear Fe(III) compound (trinuclear basic iron acetate)[22] reacting with D-(-)-quinic acid at acidic pH. On the other hand, compound **2** was synthesized and isolated at basic pH, with the base used to raise the pH being ammonia. In this latter case, a mononuclear Fe(II) compound (Mohr's salt) reacted with D-(-)-quinic acid and led to the isolation of **2**, with the (a) initially employed Fe(II) oxidized to Fe(III) and (b) the sulfate anions proving to be a crucial factor ultimately counterbalancing efficiently the positively charged species (cationic cluster and ammonium ions) and leading to the isolation of **2**. It appears, therefore, that the variable nature of the starting iron source, namely, the trinuclear iron(III) acetate or Mohr's salt instead of iron(III) nitrate, was crucial in the synthesis and isolation of the polynuclear clusters **1** and **2** bearing (a) the same nuclearity

and overall structural integrity and (b) variable OH:O^{2-} ratio. Concomitantly, the analytical, spectroscopic, and structural characterization of the isolated compounds **1** and **2**: (a) reflected their physical and chemical properties, dictated by the reaction conditions (pH and the employed trivalent or divalent form of precursor iron species), (b) revealed a considerable number of lattice structural details related to the reactivity of iron toward D-(-)-quinic acid, and (c) denoted the diversified chemical basis for the synthesis of new potential multinuclear M(II,III)−quinato species assemblies. Worth noting in the structures of **1** and **2** was (a) the oxidation state of iron with bond valence calculations, suggesting the existence of Fe(III) centers in both **1** and **2**, a contention further supported by Mössbauer spectroscopic studies, and (b) the state of deprotonation of the quinato ligand bound to Fe(III) centers. In the aforementioned metal−quinato assemblies, the alcoholic group adjacent to the carboxylic acid moiety does not retain its proton.[33,37] It appears that in the presence of various metal ions and depending on the experimental conditions in each examined binary or ternary system, the α-alcoholic group can lose or retain its proton following binding of the quinate to metal ions. A similar behavior for the α-alcoholic group was observed in the case of another α-hydroxycarboxylic acid, citric acid, which had been widely studied with various metal ions,[48,49] also leading to the formation of five-membered metallacyclic rings in diverse mononuclear and oligonuclear assemblies. Moreover, in both **1** and **2**, one of the terminal alcoholic moieties of each quinato binder is employed in the coordination to an adjacently located Fe(III) ion, thereby satisfying the octahedral coordination requirements of each Fe(III) center (also supported by Mössbauer spectroscopy). Thus, each hydroxycarboxylato binder is coordinated to two distinct iron sites in **1** and **2**. Involvement of one of the terminal alcoholic moieties in the formation of dinuclear species in binary systems has been previously observed, leading to a 1:2 metal-to-ligand ratio compounds in Mn(II),[50] Co(II),[36] and trinuclear species in Zn(II);[36] thus, suggesting that the presence of the terminal alcohols in D-(-)-quinic acid can be a key factor in the synthesis of polynuclear clusters either from binary or ternary systems, with structural differences and/or similarities compared to the aforementioned characterized materials.

Further physicochemical characterization of the two clusters in the solid state and in solution reveals that the overall structure of the two species is retained in solution as evidenced by EPR measurements. Interestingly, magnetic susceptibility measurements on the two species, supported by EPR data, showed that magnetic interactions among the Fe(III) centers can be simulated through a discrete model exemplified by similar coupling constants. Employment of such a model revealed that **1** and **2** are the first two examples of antiferromagnetic heptanuclear Fe(III) clusters with an $S = 3/2$ ground state.[26,27] It appears, therefore, that synthetic exploration of binary M(II,III)−quinato and further M(II,III)−hydroxycarboxylato systems holds promise toward oligo and polynuclear cluster assemblies, of variable yet specified magnetostructural correlations, when the aforementioned factors are taken into consideration.

Structure−Lattice Architecture and Dimensionality Correlations. The binary Fe(III)−D-(-)-quinic acid system possesses considerable diversity toward assemblies of specific lattice architectures in the solid state. This diversity is the result of the reactivity characteristics of the binary system promoting

well-defined lattices of their own composition, properties, and structural uniqueness. Previously described binary Fe(III)−quinato species[38] differentiate themselves from **1** and **2** in that they are mononuclear, thereby presenting their own unique (a) factors affecting their synthesis and isolation, pH, and reagent molar ratio and (b) lattice assembly and nature. Despite the variable metal/ligand ratio employed in the synthesis of the mononuclear and heptanuclear species, the (a) binding mode of the quinato ligand to iron through the carboxylato and alkoxido groups and (b) the coordination number around Fe(III) persists, whereas the remaining polyols enter the coordination sphere of Fe(III) only when the nuclearity of the assembled species increases from 1 to 7. The emergence of such heptanuclear assemblies does not appear to be influenced by the distinctly different charge of the two species (zero for **1** and +3 for **2**). With that in mind, the arisen Fe_7 cluster assemblies link themselves into helices which upon interjection of lattice water molecules further assemble a 3D lattice architecture (**1**), while the concurrent presence of (a) water molecules of crystallization and (b) cations (NH_4^+) and anions ($SO_4^{2−}$) raise the dimensionality of the lattice in **2** from 2D to 3D, all through hydrogen bonding interactions.

Collectively, maintenance of the coordination binding mode of quinate to Fe(III) gives rise to the same nuclearity Fe_7 cluster assemblies in **1** and **2**, where the absence or presence of charge promote distinctly different lattice architectures of the same ultimate dimensionality (3D). Auxiliary entities in the respective lattices are linked to lattice dimensionality with (a) lattice water molecules of crystallization being present as a common moiety in both lattices, regardless of the Fe_7 assembly charge (**1,2**), (b) cations and anions contributing to electroneutrality (**2**), and (c) both water molecules and charged counterions promoting higher lattice dimensionality through hydrogen bonding. It is likely that careful consideration of such factors into the assembly of distinct lattice architecture and dimensionality materials, in binary and ternary Fe(II,III)−hydroxycarboxylato systems, may give rise to new materials with distinct spectroscopic and magnetic properties. Research efforts in this direction are currently ongoing in our laboratories.

CONCLUSIONS

The pH-specific synthetic chemistry presented herein exemplifies the diversity of synthetic conditions under which the multifunctional metal ion binder D-(-)-quinic acid can lead to (a) a specific class of well-defined multinuclear binary Fe(III)−quinato species, and (b) materials with distinct physicochemical properties in the solid state and in solution. Given that an Fe(III) compound (trinuclear basic iron acetate) as well as an Fe(II) reagent (Mohr's salt) were used for the synthesis and isolation of **1** and **2**, it appears that irrespective of the pH employed, stable species eventually arose bearing the same core nuclearity yet variable oxido and hydroxido supporting bridges. In that respect, the nature of the starting Fe(III)/Fe(II) precursor used in the synthesis appears to have played a significant role in the nature of the species eventually isolated. Undoubtedly, the factors influencing the assembly nature of such a family of binary Fe(III)−quinato species, including (a) precursor nature, (b) pH, and (c) molecular stoichiometry, bear on the aqueous speciation of the investigated system and ultimately through variably promoted hydrogen bonding on the distinct lattice architecture, dimensionality and spectroscopic, electrochemical, and magnetic properties of the isolated species.

Compounds **1** and **2** represent the first examples of heptanuclear Fe7-O clusters exhibiting an overall antiferromagnetic behavior with similar exchange interactions and a ground state $S = 3/2$. Further perusal of the above factors dictating mechanistic details into the fundamental assembly of multinuclear species in this family is linked to the development of knowledge useful in the synthesis of novel materials with defined physicochemical properties and is currently under investigation in our lab.

ASSOCIATED CONTENT

Ⓢ Supporting Information

X-ray crystal crystallographic files, in CIF format, (CCDC 930734 (**1**) and 930735 (**2**)), and listings of positional and thermal parameters and H-bond distances and angles for **1** and **2**. The material is available free of charge via Internet at http://pubs.acs.org.

AUTHOR INFORMATION

Corresponding Author
*E-mail: salif@auth.gr. Fax: +30-2310-996-196. Tel.: +30-2310-996-179.

Present Address
#Department of Chemistry, Aristotle University of Thessaloniki, Thessaloniki 54124, Greece

Notes
The authors declare no competing financial interest.

ACKNOWLEDGMENTS

REFERENCES

(1) Müller, A.; Peters, F.; Pope, M. T.; Gatteschi, D. *Chem. Rev.* **1998**, *98*, 239−271.

(2) Chakov, N. E.; Zakharov, L. N.; Rheingold, A. L.; Abboud, K. A.; Christou, G. *Inorg. Chem.* **2005**, *44*, 4555−4567.

(3) Soler, M.; Wernsdorfer, W.; Sun, Z.; Huffman, J. C.; Hendrickson, D. N.; Christou, G. *Chem. Commun.* **2003**, 2672−2673.

(4) (a) Soler, M.; Wernsdorfer, W.; Folting, K.; Pink, M.; Christou, G. *J. Am. Chem. Soc.* **2004**, *126*, 2156−2165. (b) Soler, M.; Rumberger, E.; Folting, K.; Hendrickson, D. N.; Christou, G. *Polyhedron* **2001**, *20*, 1365−1369.

(5) Mandal, S. K.; Young, V. G.; Que, L., Jr. *Inorg. Chem.* **2000**, *39*, 1831−1833.

(6) Bagai, R.; Daniels, M. R.; Abboud, K. A.; Christou, G. *Inorg. Chem.* **2008**, *47*, 3318−3327.

(7) Christou, G. *Polyhedron* **2005**, *24*, 2065−2075.

(8) Na, L.; Ning, G.; Zhang, F.; Wang, B. *Front. Chem. China* **2008**, *3*, 23−26.

(9) Moro, F.; Corradini, V.; Evangelisti, M.; Biagi, R.; De Renzi, V.; Del Pennino, U.; Cezar, J. C.; Inglis, R.; Milios, C. J.; Brechin, E. K. *Nanoscale* **2010**, *2*, 2698−2703.

(10) Braun, V.; Hantke, K.; Köster, W. *Metal Ions in Biological Systems*; Sigel, H., Sigel, A., Eds.; Marcel Dekker, Inc: New York, 1998; pp 67−145.

(11) (a) Fett, J. P.; LeVier, K.; Guerinot, M. L. *Metal Ions in Biological Systems*; Sigel, H., Sigel, A., Eds.; Marcel Dekker, Inc: New York, 1998; pp 187−214. (b) Mori, S. *Metal Ions in Biological Systems*; Sigel, H., Sigel, A., Eds.; Marcel Dekker, Inc: New York, 1998; pp 215−238. (c) Jones, D. L.; Darrah, P. R.; Kochian, L. V. *Plant Soil* **1996**, *180*, 57−66. (d) Guerinot, M. L.; Yi, Y. *Plant Physiol.* **1994**, *104*, 815−820.

(12) Stojiljkovic, I.; Hantke, K. *EMBO J.* **1992**, *11*, 4359−4367.

(13) (a) Springer, B. A.; Sligar, S. G.; Olsen, J. S.; Philips, G. N. *Chem. Rev.* **1994**, *94*, 699−714. (b) Gerber, N. C.; Sligar, S. G. *J. Am. Chem. Soc.* **1992**, *114*, 8742.

(14) Yao, H.-C.; Wang, J.-J.; Ma, Y.-S.; Waldmann, O.; Du, W.-X.; Song, Y.; Li, Y.-Z.; Zheng, L.-M.; Decurtins, S.; Xin, X.-Q. *Chem. Commun.* **2006**, 1745−1747.

(15) Jones, L. F.; Low, D. M.; Helliwell, M.; Raftery, J.; Collison, D.; Aromí, G.; Cano, J.; Mallah, T.; Wernsdorfer, W.; Brechin, E. K.; Mcinnes, E. J. L. *Polyhedron* **2006**, *25*, 325−333.

(16) Hoshino, N.; Ako, A. M.; Powell, A. K.; Oshio, H. *Inorg. Chem.* **2009**, *48*, 3396−3407.

(17) Tudor, V.; Marin, G.; Lloret, F.; Kravtsov, V. C.; Simonov, Y. A.; Julve, M.; Andruh, M. *Inorg. Chim. Acta* **2008**, *361*, 3446−3452.

(18) Chen, Q.-Y.; Li, Y.; Zheng, F.-K.; Zou, W.-Q.; Wua, M.-F.; Guo, G.-C.; Wua, A.-Q.; Huang, J.-S. *Inorg. Chem. Commun.* **2008**, *11*, 969−971.

(19) Haslam, E. *Shikimic Acid: Metabolism and Metabolites*; Wiley and Sons: New York, 1993.

(20) Pittard, A. J. *Escherichia coli and Salmonella: Cellular and Molecular Biology*; Neidhardt, F. C., Ed.; ASM Press: Washington, DC, 1996; Chapter 28.

(21) Bentley, R. *Crit. Rev. Biochem. Mol. Biol.* **1990**, *25*, 307−384.

(22) Turte, K. I.; Shova, S. G.; Spatar, F. A.; Mazus, M. D.; Malinovskii, T. I. *J. Struct. Chem.* **1994**, *35*, 248−255.

(23) Rigaku/MSC. *CrystalClear*. Rigaku/MSC, Inc.: The Woodlands, TX, 2005.

(24) Sheldrick, G. M. *SHELXS-97: Structure Solving Program*, University of Göttingen: Germany, 1997.

(25) Sheldrick, G. M. *SHELXL-97: Crystal Structure Refinement*, University of Göttingen: Germany, 1997.

(26) Ako, A. M.; Waldmann, O.; Mereacre, V.; Klöwer, F.; Hewitt, I. J.; Anson, C. E.; Güdel, H. U.; Powell, A. K. *Inorg. Chem.* **2007**, *46*, 756−766.

(27) Jones, L. F.; Jensen, P.; Moubaraki, B.; Berry, K. J.; Boas, J. F.; Pilbrow, J. R.; Murray, K. S. *J. Mater. Chem.* **2006**, *16*, 2690−2697.

(28) Oshio, H.; Hoshino, N.; Ito, T.; Nakano, M.; Renz, F.; Gütlich, P. *Angew. Chem., Int. Ed.* **2003**, *42*, 223−225.

(29) Liu, T.; Wang, B.-W.; Chen, Y.-H.; Wang, Z.-M.; Gao, S. Z. *Anorg. Allg. Chem.* **2008**, *634*, 778−783.

(30) Labat, G.; Boskovicb, C.; Güdelb, H. U. *Acta Crystallogr., Sect. E* **2005**, *E61*, m611−m613.

(31) Menelaou, M.; Konstantopai, A.; Mateescu, C.; Zhao, H.; Drouza, C.; Lalioti, N.; Salifoglou, A. *Inorg. Chem.* **2009**, *48*, 8092−8105.

(32) Menelaou, M.; Mateescu, C.; Zhao, H.; Lalioti, N.; Salifoglou, A. *Polyhedron* **2009**, *28*, 883−890.

(33) Barba-Behrens, N.; Salazar-Garcia, F.; Bello-Ramirez, A. M.; Garcia-Baez, E.; Rosales-Hoz, M. J.; Contreras, R.; Flores-Parra, A. *Trans. Met. Chem.* **1994**, *19*, 575−581.

(34) Bkouche-Walksman, I. *Acta Crystallogr., Sect. C* **1994**, *50*, 62−64.

(35) Inomata, Y.; Haneda, T.; Howell, F. S. *J. Inorg. Biochem.* **1999**, *76*, 13−17.

(36) Menelaou, M.; Konstantopai, A.; Lalioti, N.; Raptopoulou, C. P.; Psycharis, V.; Terzis, A.; Mateescu, C.; Tsarhopoulos, K.; Rigas, P.; Salifoglou, A. *Inorg. Chem.* **2010**, *49*, 11449−11462.

(37) Hata, G.; Kitano, Y.; Kaneko, T.; Kawai, H.; Mutoh, M. *Chem. Pharm. Bull.* **1992**, *40*, 1604−1605.

(38) Menelaou, M.; Mateescu, C.; Zhao, H.; Rodriguez-Escudero, I.; Lalioti, N.; Sanakis, Y.; Simopoulos, A.; Salifoglou, A. *Inorg. Chem.* **2009**, *48*, 1844−1856.

(39) Deacon, G. B.; Philips, R. *J. Coord. Chem. Rev.* **1980**, *33*, 227−250.

(40) Borrás-Almenar, J. J.; Clemente-Juan, J. M.; Coronado, E.; Tsukerblat, B. S. *J. Comput. Chem.* **2001**, *22*, 985−991.

(41) Gorun, S. M.; Lippard, S. J. *Inorg. Chem.* **1991**, *30*, 1625.

(42) Hart, J. R.; Rapper, A. K.; Gorun, S. M.; Upton, T. H. *Inorg. Chem.* **1992**, *31*, 5254.

(43) Weihe, H.; Güdel, H. U. *J. Am. Chem. Soc.* **1997**, *119*, 6539.

(44) Cañada-Vilalta, C.; O'Brien, T. A.; Brechin, E. K.; Pink, M.; Davidson, E. R.; Christou, G. *Inorg. Chem.* **2004**, *43*, 5505−5521.

(45) Gatteschi, D.; Pardi, L. *Gazz. Chim. Ital.* **1993**, *123*, 231−240.

(46) (a) Richter, J.; Voigt, A. *J. Phys. A: Math. Gen.* **1994**, *27*, 1139−1149. (b) Richter, J.; Voigt, A.; Krüger, S. E.; Gross, C. *J. Phys. A: Math. Gen.* **1996**, *29*, 825−836. (c) Waldmann, O. *Phys. Rev. B* **2000**, *61*, 6138−6144.

(47) Kambe, K. *J. Phys. Soc. Jpn.* **1950**, *5*, 48−51.

(48) Matzapetakis, M.; Karligiano, N.; Bino, A.; Dakanali, M.; Raptopoulou, C. P.; Tangoulis, V.; Terzis, A.; Giapintzakis, J.; Salifoglou, A. *Inorg. Chem.* **2000**, *39*, 4044−4051.

(49) Dakanali, M.; Kefalas, E. T.; Raptopoulou, C. P.; Terzis, A.; Voyiatzis, G.; Kyrikou, I.; Mavromoustakos, T.; Salifoglou, A. *Inorg. Chem.* **2003**, *42*, 4632−4639.

(50) Menelaou, M.; Raptopoulou, C. P.; Psycharis, V.; Terzis, A.; Tangoulis, V.; Salifoglou, A. *Eur. J. Inorg. Chem.* **2006**, 1957−1967.